Modelling and Optimization of the Tube Reactors in an Ethylene Dichloride Cracker Using Pontryagin Optimal Control Theory

R. Bahrami[a], ***R. Halladj**[b].

Chemical Engineering Department, Amirkabir University of Technology, 424, Hafez Ave., Tehran, Iran, P.O.Box: 15875-4413.

Modelado y optimización de los reactores de tubos en una torre de craqueo de dicloroetileno usando la teoría de control óptimo de Pontryagin

Modelatge i optimització dels reactors de tubs en una torre de craqueig de dicloroetilè emprant la teoria de control òptim de Pontryagin

Recibido: 29 de enero de 2008; revisado: 31 de agosto de 2008; aceptado: 23 de septiembre de 2008

RESUMEN

La torre de craqueo de dicloroetileno (EDC) es el corazón de la unidad de producción de cloruro de vinilo monómero, así que predecir el comportamiento de esta torre de craqueo es algo a examinar en detalle. En este trabajo, se aplican balances de masa, energía y momento a los reactores de tubos en las torres de craqueo de dicloroetileno y las ecuaciones que se obtienen se resuelven simultáneamente usando las caracterizaciones de una unidad existente y el método numérico adecuado para predecir el comportamiento del reactor. Se obtienen los perfiles de concentración, temperatura y presión a lo largo del reactor, y se comparan con los datos de operación. En este trabajo, también se ha realizado la optimización del reactor de craqueo térmico de dicloroetileno para la producción de cloruro de vinilo monómero. La función objetiva para este problema depende de la longitud del reactor, permitiendo encontrar el perfil óptimo de temperatura de la pared externa y optimizar el perfil de la velocidad de transferencia de calor al fluido del proceso a lo largo del reactor a fin de maximizar el producto (VCM) a la salida del reactor. Las ecuaciones diferenciales de masa, energía y momento derivadas del modelado del reactor son las restricciones al problema de optimización. El presente problema se ha convertido en un problema de control óptimo usando la teoría de Pontryagin para resolverlo. Se ha utilizado Visual Fortran para la programación, y se han analizado los perfiles óptimos de estado y las variables de control como resultados del programa. Finalmente, se comparan los resultados del método usual y del método que utiliza la teoría de control óptimo de Pontryagin con los datos de operación. Este trabajo muestra que la teoría de control óptimo de Pontryagin se puede aplicar a otros casos y que en general tiene ventajas computacionales, además de precisión y robustez.

Palabras clave: **Modelado. Optimización. Dicloroetileno. Cloruro de vinilo monómero. Torre de pirólisis. Pontryagin.**

SUMMARY

Ethylene dichloride (EDC) cracker is the heart of vinyl chloride monomer (VCM) unit, so predicting the behavior of this cracker is mostly considered. In this work, mass, energy and momentum balances have been applied to the tube reactors in ethylene dichloride cracker and the obtained differential equations are solved simultaneously using the characterizations of an existing unit and the suitable numerical method to predict the reactor behavior. Profiles of concentration, temperature and pressure along the reactor have been obtained and compared with the operating data. Optimization of ethylene dichloride thermal cracking reactor for vinyl chloride monomer production has also been done in this work. The objective function for this problem depends on length of reactor which finds optimum external wall temperature profile along the reactor and can optimize the profile of heat transfer rate to the process fluid along the reactor in order to maximize the VCM product at the outlet of the reactor. Mass, energy and momentum differential equations derived from the modeling of reactor are the constraints of optimization problem. The present problem has been converted to an optimal control problem format by using the Pontryagin theory to solve it. Visual Fortran has been used for programming and optimum profiles of state and control variables have been analyzed as results of program. Finally, the results of both the usual method and the method using Pontryagin optimal theory are compared with operating data. This work shows Pontryagin optimal control theory can be applied to other cases and in general it has computational advantages, accuracy and also robustness.

Key words: **Modelling. Optimization. Ethylene dichloride. Vinyl chloride monomer. Pyrolysis cracker. Pontryagin.**

RESUM

La torre de craqueig de dicloroetilè (EDC) és el cor de la unitat de producció de clorur de vinil monòmer, així que predir el comportament d'aquesta torre de craqueig és quelcom a examinar en detall. En aquest treball, s'apliquen balanços de massa, energia i moment als reactors de tubs en la torre de craqueig de dicloroetilè i les equacions que s'obtenen es resolen simultàniament emprant les caracteritzacions d'una unitat existent i el mètode numèric adient per predir el comportament del reactor. S'obtenen els perfils de concentració, temperatura i pressió al llarg del reactor, i es comparen amb les dades d'operació. En aquest treball, també s'ha realitzat l'optimit-

---

* E-mail: halladj@aut.ac.ir

zació del reactor de craqueig tèrmic de dicloroetilè per a la producció de clorur de vinil monòmer. La funció objectiva per a aquest problema depèn de la llargada del reactor, permetent trobar el perfil òptim de temperatura de la paret externa i optimitzar el perfil de la velocitat de transferència de calor al fluid del procés al llarg del reactor per tal de maximitzar el producte (VCM) a la sortida del reactor. Les equacions diferencials de massa, energia i moment derivades del modelatge del reactor són les restriccions al problema d'optimització. El present problema s'ha convertit en un problema de control òptim emprant la teoria de Pontryagin per resoldre'l. S'ha utilitzat Visual Fortran per a la programació, i s'han analitzat els perfils òptims d'estat i les variables de control com a resultats del programa. Finalment, es comparen els resultats del mètode usual i del mètode que empra la teoria de control òptim de Pontryagin amb les dades d'operació. Aquest treball mostra que la teoria de control òptim de Pontryagin es pot aplicar a altres casos i que en general té avantatges computacionals, a més de precisió i robustesa.

Mots clau: **Modelatge. Optimització. Dicloroetilè. Clorur de vinil monòmer. Torre de piròlisi. Pontryagin.**

INTRODUCTION

Modelling can predict the behavior of a process. In many cases, prediction the parameters such as concentration and temperature can help in optimization of process. A group of differential-algebraic equations which contain mass, energy and momentum balances can explain the behavior of the process. Ethylene dichloride cracker is one of these processes which due to its importance is considered by many investigators.

Vinyl chloride monomer has vast applications in polymer industry and is produced to manufacture different plastics such as poly vinyl chloride (PVC). Vinyl chloride can be produced in different ways but most of them are not economical. The economical method is to crack ethylene dichloride to vinyl chloride in a suitable furnace at temperature 500-550 ºC and pressure 10-30 bar. The advantages of high pressure thermal cracking are: using liquid feed, enhancement of conversion, using no catalyst and smaller furnace(1).

Conversion of ethylene dichloride to vinyl chloride is about 50-55% and if this is increased to 60%, it will cause to byproducts increase. Hydrogen chloride (HCl) is main byproduct in thermal cracking of EDC but a wide range of chlorinated byproducts are produced as a result of side reactions(1).

Historically, simulation studies of hydrocarbon crackers for refinery have been conducted to upgrade the operability. These studies have been paralleled with the adaptation of a radiation model and a reaction mechanism, in which the cracker is divided into a furnace and a reaction model to identify variations in the heat supply.

In 1939, Lobo and Evans published their paper on «Heat Transfer in the Radiant Section of Petroleum Heaters», which rather accurately predicted the overall performance of the radiant section of the heaters being built at that time. The method, basically a theoretical one, was simple to use while it took into account such factors as the shape of the box, the amount of cold surface and refractory present, the properties of the fuel, the excess air, and the temperature and properties of the cold heat-receiving surface. It was based on the assumption, justified by the results, that in all the furnaces studied the mean radiating temperature could be taken as the temperature of the flue gases leaving the radiant section, obtained by heat balance, i.e. that the furnaces were essentially well-stirred boxes(2).

With the greater use of steam-hydrocarbon reforming furnaces, catalytic naphtha reformers and other processes dealing with large furnace through-puts and requiring low coil pressure drops, a new form of vertical tube heater was developed, the cellular type in which, again, tubes might be arranged along the walls and fired from one side, or arranged in the center of the cell to be fired from both sides, usually from the floor.

These new furnace shapes and types usually could not be considered as well-stirred boxes although, to a very great extent, this classification is a function of the burner flame characteristics as well as of the box dimensions, something which is seldom taken into account. Some modification or improvement in the methods of design was indicated to take into account deviations from the well-stirred-box concept and the flue gas temperature gradient which now existed(2).

In 1952, Mekler and Fairall illustrated the use of Hottel's shape factors to calculate the difference in heat flux to various tube locations in petroleum heaters, but they did not consider the temperature gradient. In 1958, Hottel and Cohen presented their zone method for radiant heat exchange making allowance for non-uniformity of gas temperatures(2). In 1967, Hottel and Sarofim simulated the firebox of the cracking furnaces(3). We developed a mathematical model for the simulation of the ethylene dichloride cracker using the multi-zone technique and assuming one dimensional conduction heat transfer in the tube reactor wall. Also, we developed a mathematical model using Pontryagin theory for the optimization of the tube reactors in a EDC cracker, especially for maximizing the vinyl chloride monomer production rate.

Reaction mechanism and kinetic parameters

Although thermal cracking real mechanism is radically but using it to design and optimize the problems increases complexity. Modelling based on radically mechanism leads to a series of differential equations which is called hard differential equations where the solutions are complicated and special. So molecular model, in fact is used for explaining thermal cracking reaction mechanism. Table I shows the main elementary reactions with their kinetic parameters in an EDC thermal cracking molecular model. The general form of kinetic equation is $r_i = k_i \frac{\Pi}{j=\text{reactant}} C_j^{v_j}$ where r_i is the i th reaction rate, k_i the rate constant of i th reaction, C_j the molar concentration of each reactant species j, v_j the molar stoichiometric coefficient for species j.

Reactor Mathematical Modelling

The EDC pyrolysis process has four conventionally distinguishable section: a radiation section, a convection section, a shock section and a stack. The radiation section,

TABLE I

Main reactions with kinetic parameters in an EDC thermal cracking molecular model(13).

Reaction	Arrhenius equation $k_i = A_{0i} \exp[\frac{-E_{0i}}{RT}]$	
	A_0	Activation energy E_0 (cal / gmol)
$1,2C_2H_4Cl_2 \xrightarrow{r_1} C_2H_3Cl+HCl$	$1 \times 10^{13.6}$	58000
$C_2H_3Cl \xrightarrow{r_2} C_2H_2+HCl$	0.5×10^{14}	69000
$1,2C_2H_4Cl_2 \xrightarrow{r_3} C_2H_4+Cl_2$	1×10^{13}	72000
$C_2H_4 \xrightarrow{r_4} C_2H_2+H_2$	0.5×10^{15}	82000

the so-called firebox contains two reactors. The heat in radiation section of the cracking furnace is transferred to reactor external surface and cracking occurs in tubular reactors which are called coil. The inside of radiation section is completely heated by burners which located on the largest two opposing walls of the firebox. The heat required for the endothermic pyrolysis reactions is supplied via the combustion of fuel from these burners. The reason why the firebox or furnace frequently referred to as radiation section is that the temperature is so high and the main heat transfer mechanism is radiation. After the radiation section, the combustion gas flows through a shock area before going to the convection section where residual heat is recovered by pre-heating the EDC feed. The combustion gas finally is emitted to the atmosphere through the stack after the convection section or heat recovery utilities, the latter of which have various forms depending to the process designs. Fig. 1 shows schematics of an EDC pyrolysis process.

Mass, energy and momentum equations are obtained in radiation section considering a cylindrical element (Fig. 2) with length dz and radius R which is the radius of tube. Whereas the flow regime is turbulent and steady state it can be assumed that no gradient in *r* and θ directions exist and so differential variations do not exist in these directions and variations are considered in z direction.

ion.

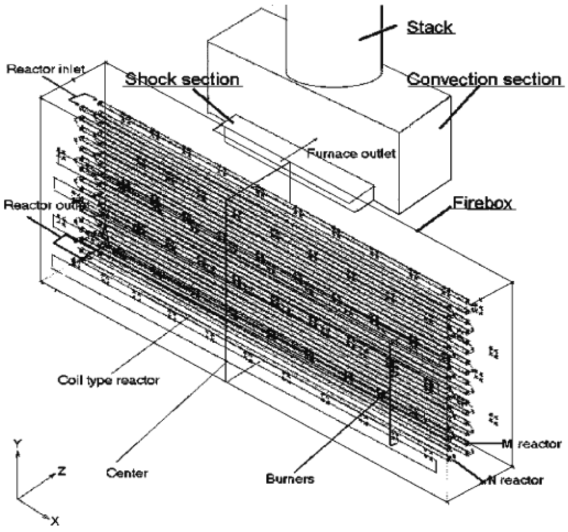

Figure 1. Schematics of an EDC pyrolysis furnace.

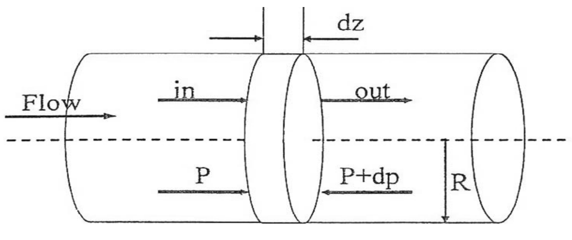

Figure 2. Cylindrical element.

Mass balance: $$\frac{dN_m}{dz} = A\sum \nu_{im} r_i \tag{1}$$

Momentum balance: $$-\frac{dp}{dz} = \left[\frac{2f}{d} + \frac{\xi}{\pi r_b}\right]\frac{G^2}{\rho} \tag{2}$$

Energy balance: $$\frac{dT}{dz} = \frac{U\pi d_0[T_w(z) - T] - \sum \Delta H^0_{fm}\frac{dN_m}{dz}}{\sum c_{pm} N_m} \tag{3}$$

In these equations, r_i is *i*th reaction rate, v_{im} is *m*th component stoichiometric coefficient in *i*th reaction, *A* is cross section area of reactor, dN_m is *m*th component molar rate, ρ is density of fluid, *G* is mass flow rate, *f* is friction factor, *d* is diameter of reactor, *U* is overall heat transfer coefficient, T_w is outside wall temperature of fluid, c_{pm} is heat capacity of *m*th component and ΔH° is enthalpy of formation.

Assumptions which are considered in reactor mathematical modelling are:

1. Temperature and concentration gradients in *r* and directions θ are negligible.
2. The steady state condition exists.
3. Plug flow is considered.
4. Coke formation is ignored in tube reactor.

Pontryagin optimal control theory(14)

In Pontryagin optimal control theory, the problem is to find an acceptable control path u^* that causes the following function:

$$\dot{x} = f(x(t),u(t),t) \tag{4}$$

minimizes the following objective function using an acceptable curve path such as x^*:

$$J(u) = h(x(t_f),t_f) + \int g(x(t),u(t),t)dt \tag{5}$$

Where $x(t_0) = x_0$ and t_0 is determined.

Therefore by defining Lagrange multiplayer, $\lambda_1(t),\ldots\ldots,\lambda_n(t)$, following relation will be introduced by using mathematical relations:

$$\int_{t_0}^{t_f}\left\{\left[\left[\frac{\partial g}{\partial x}(x^*(t),u^*(t),t)\right]^T + \lambda^{*T}(t)\left[\frac{\partial f}{\partial x}(x^*(t),u^*(t),t)\right] - \frac{d}{dt}\left[-\lambda^{*T}(t)\right]\right]\delta x(t) + \right.$$
$$\left[\left[\frac{\partial g}{\partial x}(x^*(t),u^*(t),t)\right]^T + \lambda^{*T}(t)\left[\frac{\partial f}{\partial x}(x^*(t),u^*(t),t)\right]\right]\delta u(t) +$$
$$\left.\left[\left[f(x^*(t),u^*(t),t) - x^*(t)\right]^T\right]\delta\lambda(t)\right\}dt \tag{6}$$

This integral should be zero on extermal curve by ignoring the bounding conditions. For this purpose, the constraints:

$$x^*(t) = f(x^*(t),u^*(t),t) \tag{7}$$

should be satisfied by each extermal curve and therefore the coefficient of $\delta\lambda(t)$ will be zero. Hence, the arbitrary Lagrange multiplayer should be selected such that the $x(t)$ become zero, i.e.:

$$\lambda^{*T}(t) = -\left[\frac{\partial f}{\partial x}(x^*(t),u^*(t),t)\right]^T \lambda^{*T}(t) - \frac{\partial f}{\partial x}(x^*(t),u^*(t),t) \tag{8}$$

Equation (8) is adjoint equation.

Since the constraint (4) is considered in the optimal path, Lagrange multiplayers are a function of time in general and are not a constant value such as static optimization problems. Now, only the $u(t)$ deviations have remained that should be zero because of independency of $u(t)$. Therefore:

$$\frac{\partial f}{\partial u}\left(x^*(t),u^*(t),t\right)+\left[\frac{\partial f}{\partial u}\left(x^*(t),u^*(t),t\right)\right]^T \lambda^{*T}(t)=0 \tag{9}$$

Equations (7), (8) and (9) are important equations and they are solved simultaneously for optimum condition. To investigate the boundary conditions, we can gain the following relation from the mathematical proof:

$$\begin{gathered}\left[\frac{\partial h}{\partial x}\left(x^*(t_f),t_f\right)-\lambda^*(t_f)\right]^T \delta x_f+\left[g\left(x^*(t_f),u^*(t_f),t_f\right)+\frac{\partial h}{\partial t}\left(x^*(t_f),t_f\right)+\right.\\ \left.\lambda^{*T}(t_f)\left[f\left(x^*(t_f),u^*(t_f),t_f\right)\right]\right]\delta t_f=0\end{gathered} \tag{10}$$

Now, we define Hamiltonian function H as following equation:

$$H\left(x^*(t),u^*(t),\lambda^*(t),t\right)=+g\left(x^*(t),u^*(t),t\right)+\lambda^*(t),f\left(x^*(t),u^*(t),t\right) \tag{11}$$

Equations (7), (8), (9) and (10) are transformed to following relations:

$$x^*=\frac{\partial H}{\partial \lambda}\left(x^*(t),u^*(t),\lambda^*(t),t\right)=f\left(x^*(t),u^*(t),t\right)) \tag{12}$$

$$\lambda^*(t)=\frac{\partial H}{\partial x}\left(x^*(t),u^*(t),\lambda^*(t),t\right) \tag{13}$$

For $t\in[t_0,t_f]$ we have:

$$\frac{\partial H}{\partial u}\left(x^*(t),u^*(t),\lambda^*(t),t\right)=0 \tag{14}$$

And also:

$$\begin{gathered}\left[\frac{\partial h}{\partial x}\left(x^*(t_f),t_f\right)-\lambda^*(t_f)\right]^T \delta x_f+\\ \left[H\left(x^*(t_f),u^*(t_f),\lambda^*(t_f),t_f\right)+\frac{\partial h}{\partial x}\left(x^*(t_f),t_f\right)\right]\delta t_f=0\end{gathered} \tag{15}$$

Steepest descent algorithm for minimizing the functions (Gradient method) now is used to solve the following differential equations and it is assumed that the control curve $u^i(t)$, $t\in[t_0,t_f]$ is determined:

$$\dot{x}^{(i)}(t)=f\left(x^{(i)}(t),u^{(i)}(t),t\right) \tag{16}$$

$$\dot{\lambda}^{(i)}(t)=-\frac{\partial H}{\partial x}\left(x^{(i)}(t),u^{(i)}(t),\lambda^{(i)}(t),t\right) \tag{17}$$

Such that the state - adjoint paths curve $\lambda^{(i)},x^{(i)}$ satisfy the boundary conditions:

$$\lambda^{(i)}(t)=\frac{\partial h}{\partial x}\left(x^{(i)}(t_f)\right) \qquad x^{(i)}(t_0)=x_0 \tag{18}$$

Furthermore, if this control curve satisfy the following relation, then $u^{(i)}(t)$, $\lambda^{(i)}(t)$ and $x^{(i)}(t)$ will be the extermal curve:

$$\left[\frac{\partial H}{\partial u}\left(x^{(i)}(t),u^{(i)}(t),\lambda^{(i)}(t),t\right)=0 \qquad t\in[t_0,t_f] \tag{19}$$

Consider above definitions, steepest descent algorithm is represented as follows:

1 - An approximation for control curve $u^{(0)}(t)$ for each $t\in[t_0,t_f]$ is selected and stored in computer memory. For example we can do this operation by dividing the time range to N (often equal) partition:

$$u^{(0)}(t)=u^{(0)}(t_k) \qquad t\in[t_k,t_{k+1}] \qquad k=0,1,\ldots\ldots,N-1) \tag{20}$$

Iteration index is supposed zero.

2 - using $u^{(i)}(t)$, state equations are integrated from t_0 to t_f with considering $x(t_0)=x_0$ and using forth degree of range-kuta method and store the obtained state path curve $x^{(i)}$ as vector function.

3 - By alternating $x^{(i)}(t_f)$ from second step in equation (18), the value of $\lambda^{(i)}(t_f)$ can be calculated and store it as initial condition. Stored values of $x^{(i)}$ can be used to integrate the adjoint equation from t_0 to t_f using forth degree of range-kuta method.

The values of $\frac{\partial H(t)^{(i)}}{\partial u}$ for $t\in[t_0,t_f]$ are also calculated and stored.

4 - The following relation is calculated:

$$d=\left\|\frac{\partial H^{(i)}}{\partial u}\right\|^2=\int_{t_0}^{t_f}\left[\frac{\partial H^{(i)}}{\partial u}(t)\right]^T\left[\frac{\partial H^{(i)}}{\partial u}(t)\right]dt \tag{21}$$

And if the relation:

$$d\leqslant\gamma \tag{22}$$

be held (where γ is a positive small constant), iteration method is terminated and state and control variables are considered as the output program.

If the equation (22), that is the termination condition, not to be held, a new approximation for control curve is generated as:

$$u^{(i+1)}(t_k)=u^{(i)}(t_k)-\tau\,\frac{\partial H^{(i)}}{\partial u}(t_k) \qquad k=0,1,\ldots\ldots,N-1 \tag{23}$$

Where:

$$u^{(0)}(t)=u^{(0)}(t_k) \qquad t\in[t_k,t_{k+1}] \qquad k=0,1,\ldots\ldots,N-1) \tag{24}$$

And τ is the step size that can be supposed constant.
Now, we alternate $u^{(i)}(t_k)$ by $u^{(i+1)}(t_k)$ (for $k=0,1,\ldots\ldots,N-1$) and go to step 2.
We use the explained gradient method, (that causes solution of the problem by Pontryagin minimum principle), for solving the EDC pyrolysis reactor problem. First, we should formulize the problem such as Pontryagin formulation. EDC pyrolysis reactor system have a set of first-order differential equations such as (1), (2) and (3) equations that have been obtained from mass, momentum and energy balances in reactor mathematical modelling section.
If we choose VCM product maximizing in the outlet of reactor as the objective function, we should find an optimum temperature profile for the reactor tubes' wall. Therefore the objective function is as follows:

$$MAX_{T_w} \qquad J=N_{VCM}\Big|_{z=L} \tag{25}$$

With regard to standard Pontryagin minimum principle theory, the negative of the objective function should be minimized in order to maximize it. So the final form of optimization will be as follows:

$$MAX_{T_w} \qquad J=-N_{VCM}\Big|_{z=L} \tag{26}$$

For simplification, we use alternative variables as follow:

$$\frac{dN_j}{dz}=f_j \qquad j=1,2,\ldots 7 \tag{27}$$

Since, we have seven types of component, *j* is varied from 1 to 7.

$$\frac{dP}{dz} = f_8 \tag{28}$$

$$\frac{dT}{dz} = f_9 \tag{29}$$

Here, the control variable is T_w. So:

$$u = T_w \tag{30}$$

Now, by using equation (5) and by comparing it with exiting objective function, we consider there is not the integral expression here. So if we use definition of equation (11) for forming Hamiltonian function then we will obtain the following relation:

$$H = \vec{\lambda}^T (z).\vec{f}(\vec{x}, u, z) \tag{31}$$

Here, $\vec{\lambda}(z)$ is Lagrange multipliers vector corresponding to differential constraints which are held in the system. Now if we use equation (12) then we will obtain the following relation:

$$\dot{\vec{x}} = \frac{d\vec{x}}{dz} = \frac{\partial H}{\partial \vec{\lambda}} = \vec{f} \tag{32}$$

Equation (32) is the system state equations. In other hand, using equation (10), we define the adjoint equations as follow:

$$\dot{\vec{\lambda}} = \frac{d\vec{\lambda}}{dz} = \frac{\partial H}{\partial \vec{x}} = -\vec{\lambda}^T (z).\frac{\partial \vec{f}}{\partial \vec{x}} \tag{33}$$

And finally equation (14) is formed as follow:

$$\frac{\partial H}{\partial u} = \vec{\lambda}^T (z).\frac{\partial f}{\partial u} = \vec{\lambda}^T (z).\frac{\partial f}{\partial T_w} = 0 \tag{34}$$

Visual Fortran is used for programming and optimum profiles of state and control variables are analyzed as results of program.

RESULTS AND DISCUSSION

In this section by using the operating data of EDC pyrolysis reactor characteristics extracted from existing unit in Abadan Petrochemical Complex, the results of programming are analyzed. Table II shows the characteristics of this EDC cracker.

– Temperature

Figures 3 and 4 show fluid temperature profiles as a function of reactor length in two states of optimized and non optimized, respectively. In both profiles, temperature increases with high rate at the beginning of tube but then the slope decreases. The reason is that the cracking reaction has not begun at first and heat transferred to reactor causes to increase fluid temperature, so the temperature increases quickly but then with beginning of endothermic cracking reactions, it absorbs the heat and temperature will not go high sharply as before.

The existing difference in two profiles is higher temperature at the end of reactor in optimum state. Fluid temperature at the end of reactor in optimum state is 835 K whereas it is 814 K in non optimum state.

TABLE II

EDC pyrolysis reactor characteristics from existing unit in Abadan Petrochemical Complex.

Furnace dimensions	Length = 9305 mm Height = 4465 mm Depth = 2680 mm
Furnace length	300 m
Tube inlet diameter	10.16 cm
Thickness	1 cm
Mean length of each tube	8.57 m
Number of tube passes	35
Row in front of burner	1
Center to center distance of tubes	22.32 cm
Inlet temperature to reaction zone	2300 KPa
Reactor outlet temperature	810.9 K
Inlet pressure to reaction zone	810.9 K
Allowed pressure drop	412-2160 KPa
Feed flowrate	37.8 mol/s
Conversion percent	%53
Type of fuel	Natural gas
Excess air percent	%15
Pressure of inside radiation zone	5 psig
Reactor tubes material	Incoloy 800
Heat conductivity at 20ºC	14.6 w/m.K

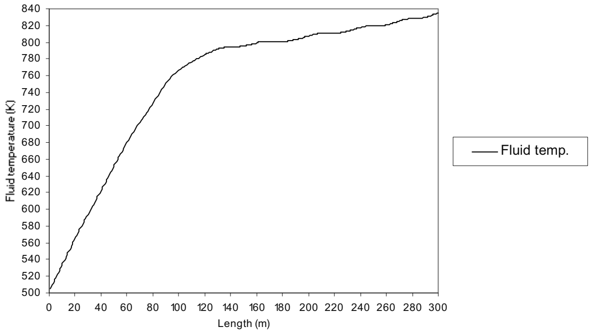

Figure 3. Fluid temperature profile as a function of reactor length in optimized state.

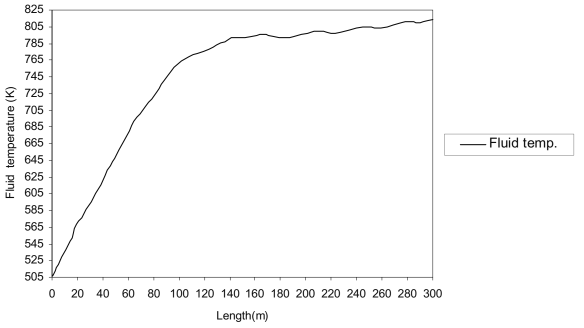

Figure 4. Fluid temperature profile as a function of reactor length in non optimized state.

– Tube reactor external wall temperature

Figures 5 and 6 show reactor external wall temperature profiles as a function of reactor length in two states of optimized and non optimized, respectively. In both figures, fluctuations exist in profiles. These fluctuations are due to existing tube passes which generally will depend on arrangement of tubes in the furnace. It is also observed in both figures that as we more approach the end of reactor, the reactor external wall temperature increases more. The reason is that, the fluid inside tube has low temperature at first and much more heat is transferred from tube wall to fluid, so wall temperature decreases but then fluid temperature increases and heat transferred from wall to fluid at the end of reactor is less than that in the beginning of reactor, as a result heat of furnace causes to increase tube external wall temperature.

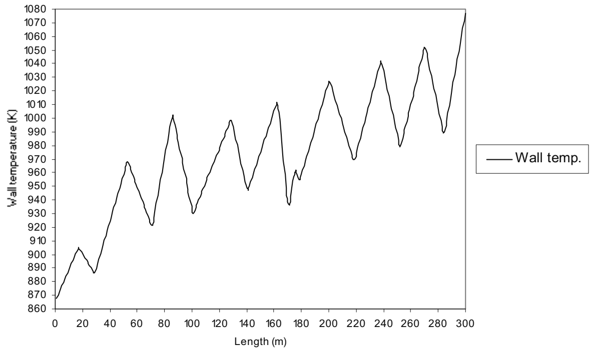

Figure 5. Reactor external wall temperature profile as a function of reactor length in optimized state.

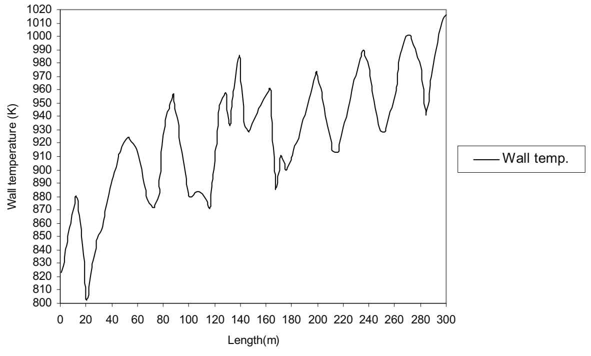

Figure 6. Reactor external wall temperature profile as a function of reactor length in non optimized state.

– Pressure

Figures 7 and 8 show pressure profiles as a function of reactor length in two states of optimized and non optimized, respectively. Comparing these figures shows that pressure drop in state of optimum is more than that of non optimum but the trend of pressure profile in both states is the same. The reason is that mechanical shape and essentially mechanical design of tube reactor in both states has been considered the same. In other words, figure and sum bends in both states is the same.

– Conversion

Figures 9 and 10 show molar flowrate profiles of ethylene dichloride and vinyl chloride monomer as a function of reactor length in two states of optimized and non optimized,

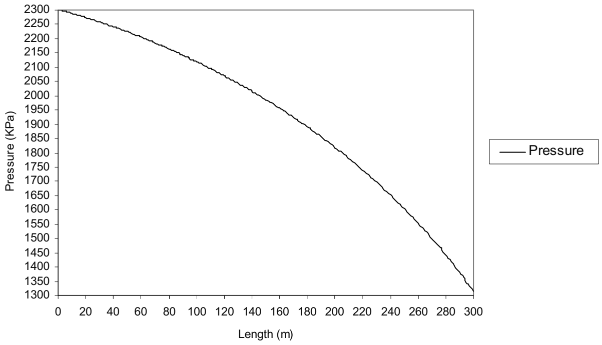

Figure 7. Pressure profile as a function of reactor length in optimized state.

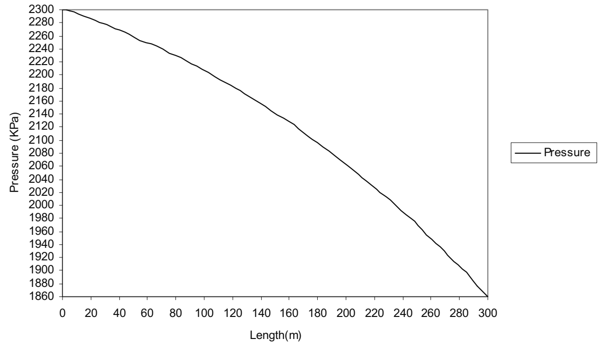

Figure 8. Pressure profile as a function of reactor length in non optimized state.

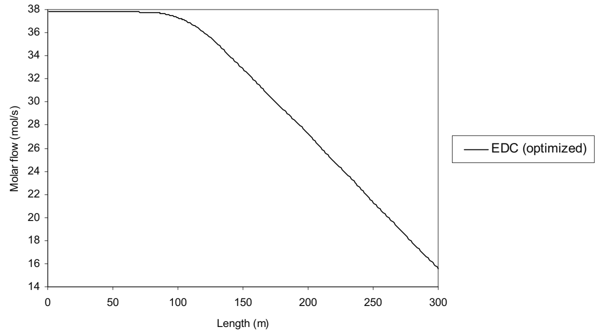

Figure 9. EDC molar flow profile as a function of reactor length in optimized state.

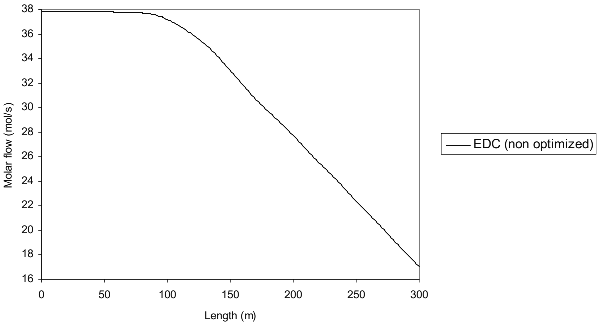

Figure 10. EDC molar flow profile as a function of reactor length in non optimized state.

respectively. In both profiles, in the beginning, the molar flows are constant because the cracking reaction has not begun yet and so heat transferred to reactor causes to increase fluid temperature but after that the change will occur and ethylene dichloride flowrate decreases whereas the vinyl chloride flowrate increases. This confirms the temperature profile that the cracking reaction begins after a while.

Existing difference in these figures is due to ethylene dichloride conversion to vinyl chloride which is higher in optimum state and naturally, vinyl chloride flowrate in optimum state is more than that of non optimum. In other words, conversion of ethylene dichloride in optimum state is more than that of non optimum.

– Heat flux

Figures 11 and 12 show transferred heat flux profiles as a function of reactor length in two states of optimized and non optimized, respectively. In this figures, two points are in common: first, the causes of existing fluctuations in these profiles are the same as that of tube reactor external wall temperature. Second, generally heat flux begins from high levels and after some reduction it becomes almost fix but then somewhat increases again. The reason is that at the beginning of reactor, high temperature gradient exists between inside and outside of tube reactor and as we approach more to the end of reactor, temperature gradient becomes less, but because of the beginning of side reactions at the end of reactor, heat transferred to reactor increases due to their required heat.

Existing difference in these figures is due to heat flux transferred to reactor in optimum state which is higher than that of non optimum. In other words, in figure 9 maximum and minimum heat flux are $136\frac{KW}{m^2}$ and $69\frac{KW}{m^2}$, respectively. Whereas in figure 10 they are $113\frac{KW}{m^2}$ and $44\frac{KW}{m^2}$.

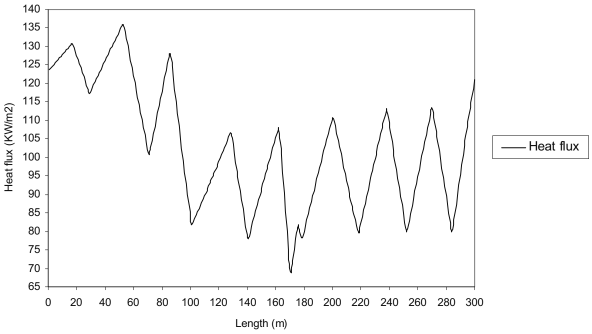

Figure 11. Heat flux profile as a function of reactor length in optimized state.

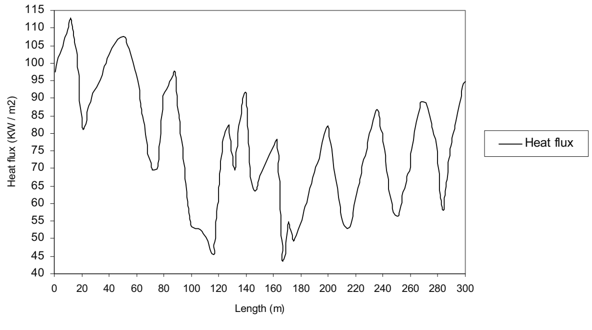

Figure 12. Heat flux profile as a function of reactor length in non optimized state.

CONCLUSIONS

Conversion of ethylene dichloride to vinyl chloride monomer is increased by using Pontryagin optimization method. Comparing the results obtained from modelling and optimization with Abadan Petrochemical Complex operating data show a good agreement. Table III presents this comparison.

TABLE III

Comparison of obtained results with operating data.

Method / Parameter	Simulation Results	Operating Data	Optimization Results	Error %
Outlet Temperature (K)	814	811	835	0.369
Pressure Drop (KPa)	440	412 –2160	985	0
Conversion of feed(%)	55	53	58.6	3.63

Also modelling and Pontryagin optimal theory show:

1. In both optimized and non optimized states, temperature increases with high rate at the beginning of tube but then these decreases. The existing difference between two profiles is the higher temperature at the end of reactor in optimum state.
2. In both optimized and non optimized states, fluctuations exist in reactor external wall temperature profiles. It is also observed in both figures that as we more approach the end of reactor, the reactor external wall temperature increases more. Fluctuations are due to arrangement of tubes.
3. Comparing pressure profiles of optimized and non optimized states shows that pressure drop in optimized state is more than that of non optimized but the trend of pressure profile in both states is the same.
4. In both flowrate profiles of ethylene dichloride and vinyl chloride monomer in two states of optimized and non optimized, in the beginning, the molar flows are constant because the cracking reaction has not begun yet but after that the change will occur and ethylene dichloride flowrate decreases whereas the vinyl chloride flowrate increases. Existing difference between these profiles is due to ethylene dichloride conversion to vinyl chloride which is higher in optimized state and naturally, vinyl chloride flowrate in optimized state is more than that of non optimum. In other words, conversion of ethylene dichloride in optimized state is more than that of non optimum. It should be also mentioned that the goal of this work was to optimize the production rate of EDC.
5. Heat flux profiles in two states of optimized and non optimized, are common in two points: first, fluctuations exist in both profiles. Second, heat flux generally begins from high levels and after some reduction it becomes almost fix but then somewhat increases again. Existing difference between these profiles is due to higher heat flux transferred to reactor in optimized state. As the same of external wall temperature, fluctuations are due to arrangement of tubes and the differences between the heat fluxes obtained from optimized and non optimized results in length of 100 to 180 m is due to difference of wall temperature in this distance, because the heat fluxes are functions of wall temperature and we see the same difference in wall temperature.

Notation

C_p	heat capacity, J/mole.K
d	reactor diameter, m
N_m	molar flow rate, mole/s
ΔH_f	enthalpy of formation, J/mole
P	total pressure, Pa
Q	heat flux, W/m^2
r_b	radius of the tube bend, m
r_i	reaction rate in pyrolysis process, $mole/m^3.s$
υ_{ji}	stochiometry factor
T	fluid temperature, K
u	control variable
τ	Pitch
f	friction factor
G	mass flow rate
ζ	supplementary pressure drop, Pa
z	axial coordinate, m
λ	Lagrange multiplayer
ρ	fluid density, kg/m^3

BIBLIOGRAPHY

(1). Wong, E.W.; Ambler, C.P. «Produce high purity VCM product». *Hydrocarbon Processing*, pp. 129-132, 1992.

(2). Lobo, W.E. «Design of furnaces with flue gas temperature gradients». *Chemical Engineering Progress*, **70**, pp. 65-71, 1974.

(3). Hottel, H.C.; Sarofim, A.F. «Radiative Transfer», New York: Mc Graw-Hill, 1993.

(4). Biegler, L.T.; Cervantes, A.M. «A stable elemental decomposition for dynamic process optimization». *J. Computational and Applied Mathematics*, **120**, pp. 41-57, 2000.

(5). Kirk-Othmer: Encyclopedia of chemical technology, 4th edition, Volume 24, John Wiley & Sons.

(6). Plehiers, P.M.; Reyniers, G.C.; Froment, G.F. «Simulation of the run length of an ethane cracking furnace». *Industrial Engineering & Chemistry Research*, **29**, pp. 636-641, 1990.

(7). Detemmerman, T.; Froment, G.F. «Three dimensional coupled simulation of furnaces and reactor tubes for the thermal cracking of hydrocarbons». *Revue De L'Institut Francais du Petrole*, **53**, pp. 181-194, 1998.

(8). Wozney, G.; Li, P. «Planning and optimization of dynamic plant operation». *Applied Thermal Eng.*, **20**, pp. 1393-1407, 2002.

(9). Rao, M.V.R.; Plehiers, P.M.; Froment, G.F. «The coupled simulation of heat transfer and reaction in a pyrolysis furnace». *Chem. Eng. Sci.*, **43**, pp. 1223-1229, 1988.

(10). Chen, C.L.; Sun, D.Y.; Chang, Y.C. «Numerical solution of dynamic optimization problems with flexible inequality constraints by iterative dynamic optimization». *Fuzzy Sets and System*, **127**, pp. 167-176, 2002.

(11). Edgar, T.F.; Himmelblau, D.M. «Optimization of chemical processes». New York: Mc Graw-Hill, 2001.

(12). Storen, S.; Hertzberg, T. «Obtaining sensitivity information in dynamic optimization problems solved by the sequential approch». *Comp. & Chem. Eng.*, **23**, pp. 807-819, 1999.

(13). Tong, W.H.; Liu, G.R. «An optimization procedure for truss structures with discrete design variables and dynamic constraints». *Computer & Structures*, **79**, pp. 155-162, 2001.

(14). Lakshmanan, A.; Rooney, W.C.; Biegler, L.T. «A case study for reactor network synthesis: the vinyl chloride process», 1998.

(15). Kirk, D.E. «Optimal control theory», London: Prentice-Hall, 1990.

(16). Li, P.; Wendt, M.; Arellano-Garcia, H. «Optimal operation of distillation processes under uncertain inflows accumulated in a feed tank». *AICHE J.*, **48**, pp. 1198-1211, 2002.

(17). Levenspiel, O. «Chemical Reaction Engineering»: John Wiley & Sons, 2000.

(18). Lee, J.K.; Kang, K.H.; Song, K.H. «Increase VCM output». *Hydrocarbon Processing*, pp. 63-66, 2001.

(19). Huang, J.Y.; Reklaitis, G.V.; Venkatasubramanian. «Model decomposition based method for solving general dynamic optimization problems». *Comp &. Chem. Eng.*, **26**, pp. 863-873, 2002.

(20). Nath, R.; Alzein, Z. «Dynamic optimization of olefins plants». *Comp &. Chem. Eng.*, **24**, pp. 533-538, 2000.

(21). Raha, S.; Petzold, L.R. «Constraint partitioning for structure in path-constrained dynamic optimization problems». *Applied Numerical Mathematics*, **39**, pp. 105-126, 2001.